AD-A062 253   STATE UNIV OF NEW YORK AT BUFFALO DEPT OF ENGINEERIN--ETC F/G 20/11
                SOME RESULTS ON THE ONE-DIMENSIONAL COUPLED NONLINEAR THERMOVIS--ETC(U)
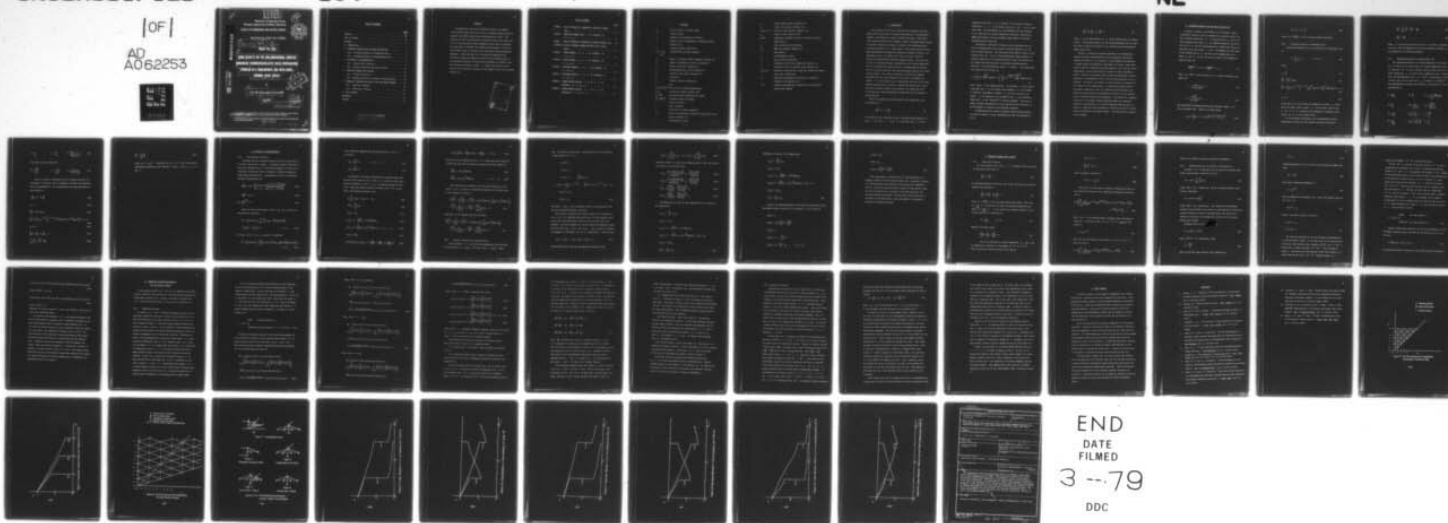   JUL 78   C LEE, W P CHANG, F A COZZARELLI   N00014-75-C-0302
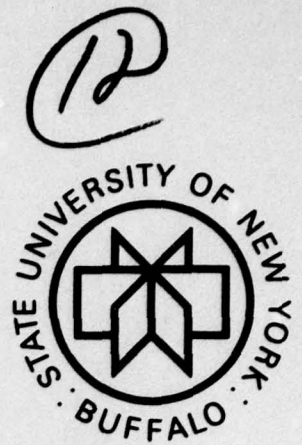UNCLASSIFIED   104   NL

|OF|
AD
A062253

END
DATE
FILMED
3 -- 79
DDC

LEVEL

Department of Engineering Science,
Aerospace Engineering and Nuclear Engineering

FACULTY OF ENGINEERING AND APPLIED SCIENCES

STATE UNIVERSITY OF NEW YORK · BUFFALO ·

State University of New York at Buffalo

(9) Summary rept., (14)

Report No. 104

(6)

SOME RESULTS ON THE ONE-DIMENSIONAL COUPLED NONLINEAR THERMOVISCOELASTIC WAVE PROPAGATION PROBLEM IN A SEMI-INFINITE ROD WITH FINITE THERMAL WAVE SPEED*,
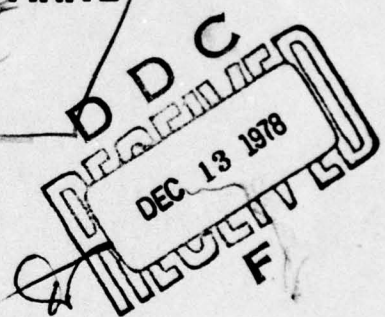
DDC
DEC 13 1978
F

by

(10)

C. Lee, W.P. Chang and F.A. Cozzarelli**

(11) July, 1978

(12) 51 p.

406156

78 12 11 015

TABLE OF CONTENTS

ABSTRACT

One-dimensional stress and temperature fields in a suddenly
loaded and/or heated semi-infinite rod of nonlinear thermoviscoelastic
material are studied using coupled thermomechanical theory. The
transport of heat is governed by the modified Fourier heat conduction
law, and thus proceeds by wave propagation rather than by diffusion.
The application of thermal and mechanical disturbances at the end of
the rod gives rise to two wave fronts along which these disturbances
propagate. Field solutions for the stress and temperature are
obtained by numerical integration along the five characteristics of
the governing equations, and results are presented for several linear
and nonlinear viscoelastic models. A closed form solution is also
obtained via the Laplace transform for the special case of an uncoupled
thermal wave.

LIST OF FIGURES

NOTATION

C_σ	specific heat at constant stress
E	Young's modulus
J	integer as an indication of position
K	integer for the condensation of computer storage, Equation (42)
k	isotropic thermal conductivity
$k_i = \dfrac{1}{\tau_i \mu_i}^{q_i}$	nondimensional material constants
M	number of nonlinear memory integrals, Equation (2)
N	number of components of strain, Equation (7)
n	steady creep power, Equation (2)
Q	one-dimensional heat flux, Equation (1)
q_i	transient creep powers, Equation (2)
T	temperature
T_o	constant reference temperature
t	time
$t_s = (\lambda/E)^n / \bar{\sigma}_o^{n-1}$	time scale for nondimensionalization
V_1, V_2	coupled wave speeds, Equation (6a)
$V_e = \sqrt{E/\rho}$	uncoupled elastic mechanical wave speed
$V_T = \sqrt{k/\rho C_\sigma \tau}$	uncoupled thermal wave speed
v	particle velocity
x	space coordinate
α	coefficient of thermal expansion
γ, δ	positive nondimensional quantities governing the wave speeds, Equations (5)
ε	one-dimensional strain

ϵ_1	linear elastic strain, Equation (7b)
ϵ_2	steady creep strain, Equation (7c)
$\epsilon_i, i=3,\ldots,N$	transient creep strains, Equation (7d)
ϵ_T	thermal strain, Equation (7e)
$\theta = T - T_o$	temperature increment relative to constant reference temperature T_o
θ_o	input temperature discontinuity
λ, μ_i	material constants, Equation (2)
ρ	mass density
σ	one-dimensional stress
σ_o	input stress discontinuity
τ	relaxation time of heat conduction, Equation (1)
τ_i	retardation time of transient creep, Equation (2)
$[\ ]_j, j=1,2$	indicates a discontinuity across the leading and lagging wave fronts respectively
$(\tilde{\ })$	indicates nondimensional variables and parameters (dropped after Equation (9))
$(\ )^*$	indicates nondimensional variables for the uncoupled thermal wave problem

1. INTRODUCTION

The classical Fourier heat conduction law is based on the hypo-
thesis that the heat flux is linearly proportional to the temperature
gradient, and predicts an infinite thermal wave speed. This physi-
cally anomalous behavior has prompted a number of proposed modifications
to the heat conduction law which can predict two thermomechanically
coupled wave speeds (i.e., second sound.) The second sound effect has
been experimentally observed and extensively studied in solids at low
temperatures (e.g., see Rogers [1]), and it has been noted that
second sound disturbances experience damping effects. From the point
of view of continuum mechanics, damping may result from an additional
term in a modified heat conduction law, a thermomechanical coupling
term in the energy equation, and from viscoelastic terms in the consti-
tutive relation. The relative importance of these three damping
mechanisms may vary with temperature, but they are in general all
present. It is our primary goal to demonstrate that even if all these
damping mechanisms are included in a general way resulting in a very
difficult nonlinear boundary value problem, the problem may still
be successfully treated numerically through the use of the method of
characteristics.

Chester [2] employed a modified Fourier heat conduction law in
one-dimension as

$$\tau \frac{\partial Q}{\partial t} + Q = - k \frac{\partial \theta}{\partial x} \tag{1}$$

and showed that the temperature obeys a dissipative wave equation in
space x and time t. In (1) Q is the heat flux, θ is the

temperature difference $T - T_o$ relative to the constant reference temperature T_o, k is the thermal conductivity and τ is the relaxation time. Lord and Shulman [3], and Achenbach [4] have employed (1) to study waves in linear thermoelastic materials, and recently Chang and Cozzarelli [5] have extended these results to nonlinear thermoviscoelastic materials.

Viscoelastic constitutive relations may be developed from the laws of thermodynamics by the energy functional approach or by the state variable approach. Both approaches yield similar results as discussed by Cost [6]. In [5] a three-dimensional single integral constitutive equation, of the generalized Kelvin type, was obtained via the energy functional approach for nonlinear thermoviscoelastic materials. For one-dimensional stress σ, strain ε and temperature, this relation may be written as

$$\varepsilon = \frac{\sigma}{E} + \int_0^t (t-t') \frac{\partial \left|\frac{\sigma}{\lambda}\right|^n}{\partial t'} \, \text{sgn}(\sigma) dt' + \int_0^t \sum_{i=1}^{M} (1-e^{\frac{-(t-t')}{\tau_i}}) \frac{\partial \left|\frac{\sigma}{\mu_i}\right|^{q_i}}{\partial t'} \, \text{sgn}(\sigma) dt' + \alpha\theta$$

(2)

where $\text{sgn}(\sigma)$ is the signum function. In the above n is the steady creep power and λ is the steady creep parameter; M is the number of transient creep memory integrals, q_i are the transient creep powers, μ_i are transient creep parameters and τ_i are retardation times; and α is the coefficient of thermal expansion. This kind of single integral representation is quite general and is convenient for the development of analytical and numerical solutions.

A thermomechanically coupled linearized energy equation identical with the result of linear thermoelasticity was also obtained in [5] as

$$\frac{\partial Q}{\partial x} + \alpha T_o \frac{\partial \sigma}{\partial t} + \rho C_\sigma \frac{\partial \theta}{\partial t} = 0 \tag{3}$$

where ρ is the mass density and C_σ is the specific heat at constant stress. In obtaining Equation (3) the energy dissipation and the thermal kinetic energy (see Kaliski [7] for details) have been dropped as higher order terms.

Section 2 contains the governing equations of one-dimensional coupled nonlinear thermoviscoelastic wave propagation with finite thermal wave speed, for the problem of a semi-infinite rod subjected to sudden thermal and mechanical disturbance at its end. These equations include the previously discussed equations (1-3) plus the strain-displacement relation and equation of motion for small deformation theory. Using the prescribed initial values and appropriate reference quantities, a nondimensional form of the governing equations is also obtained. In section 3 the method of characteristics is presented in full detail for the problem posed. A closed form solution based on the Laplace transform as well as a numerical solution based on the method of characteristics are presented in section 4 for the special case of uncoupled thermal wave propagation. The details of a numerical procedure for the general problem employing numerical integration along five characteristics in a finite difference mesh are given in section 5, along with some discussion of numerical results for several linear and nonlinear viscoelastic models. The final section contains a brief summary.

2. GOVERNING EQUATIONS FOR THE SEMI-INFINITE ROD

Consider a straight, semi-infinite rod of nonlinear thermo-viscoelastic material, which is assumed to be initially stress free and at uniform temperature T_o. A constant stress σ_o and a constant temperature increment θ_o are suddenly applied at the end of the rod ($x = 0$), and two thermomechanically coupled wave fronts are generated along the positive x axis. We designate the wave speed of the leading wave by V_1 and that of the lagging wave by V_2, where V_1 and V_2 are the two positive roots of the biquadratic equation (see [5])

$$\left(\frac{dx/dt}{V_e}\right)^4 - (1 + \delta + \gamma)\left(\frac{dx/dt}{V_e}\right)^2 + \gamma = 0 \tag{4}$$

Here, $V_e = \sqrt{E/\rho}$ is the uncoupled ($\alpha = 0$) elastic mechanical wave speed, and

$$\gamma = \frac{\rho k}{E\tau(\rho C_\sigma - T_o E\alpha^2)} > 0 \tag{5a}$$

$$\delta = \frac{T_o E\alpha^2}{\rho C_\sigma - T_o E\alpha^2} \geq 0 \tag{5b}$$

are non-negative nondimensional material constants, where $\delta = 0$ is the uncoupled case. Equation (4) then yields

$$V_{1,2} = V_e\left[\frac{1}{2}(1 + \delta + \gamma) \pm \frac{1}{2}\sqrt{(1 + \delta + \gamma)^2 - 4\gamma}\right]^{1/2} \tag{6a}$$

$$V_1 \geq V_T > V_e \geq V_2 \qquad \qquad (6b)$$

where $V_T = \sqrt{K/\rho C_\sigma \tau}$ is the uncoupled thermal wave speed.

2(a).   Governing Equations in Dimensional Form

Constitutive equation (2) may be rewritten in differential form as

$$\varepsilon = \sum_{i=1}^{N} \varepsilon_i + \varepsilon_T \qquad , \quad N = M + 2 \qquad \qquad (7a)$$

where

$$\varepsilon_1 = \frac{\sigma}{E} \qquad \qquad (7b)$$

$$\frac{\partial \varepsilon_2}{\partial t} = \left| \frac{\sigma}{\lambda} \right|^n \mathrm{sgn}(\sigma) \qquad \qquad (7c)$$

$$\frac{\partial \varepsilon_i}{\partial t} = \frac{1}{\tau_i} \left[-\frac{1}{\tau_i} e^{-t/\tau_i} \int_0^t e^{-t'/\tau_i} \left| \frac{\sigma}{\mu_i} \right|^{q_i} \mathrm{sgn}(\sigma) dt' + \left| \frac{\sigma}{\mu_i} \right|^{q_i} \mathrm{sgn}(\sigma) \right], i=3,\ldots,N \qquad (7d)$$

$$\varepsilon_T = \alpha\theta \qquad \qquad (7e)$$

In the above N is the number of components of strain, ε_1 represents the linear elastic strain, ε_2 is the steady creep strain, ε_i for $i = 3,\ldots,N$ represents the components of transient creep strain, and ε_T is the thermal strain.

For infinitesimal deformation, the one dimensional strain-displacement relation and the equation of motion are given by

$$\frac{\partial \varepsilon}{\partial t} = \sum_{i=1}^{N} \frac{\partial \varepsilon_i}{\partial t} + \frac{\partial \varepsilon_T}{\partial t} = \frac{\partial v}{\partial x} \tag{8a}$$

$$\frac{\partial \sigma}{\partial x} = \rho \frac{\partial v}{\partial t} \tag{8b}$$

where v is the particle velocity in the x direction. Equations (1,3,7,8), with the appropriate initial and boundary conditions, are the complete set of governing equations.

2(b).   Governing Equations in Nondimensional Form

For nondimensionalization the initial magnitude of the stress $|\sigma_o|$ is used for the stress scale, the coupled lagging wave speed V_2 [Equation (6)] is used to define a velocity scale, and the reference temperature T_o is chosen as the temperature scale. Furthermore, the nondimensional factor $\bar{\sigma}_o = |\sigma_o|/E$ is introduced to yield a strain scale, and the time scale t_s is taken as $(\lambda/E)^n/\bar{\sigma}_o^{n-1}$. The nondimensional variables and parameters as indicated by a bar are then defined as

$$\bar{x} = \frac{x}{V_2 t_s} \qquad\qquad \bar{\theta} = \frac{\theta}{T_o} \qquad\qquad \bar{\mu}_i = \frac{\mu_i}{(E|\sigma_o|^{q_i-1})^{1/q_i}}$$

$$\bar{t} = \frac{t}{t_s} \qquad\qquad \bar{Q} = \frac{Q}{V_2 \bar{\sigma}_o |\sigma_o|} \qquad\qquad \bar{C}_\sigma = \frac{C_\sigma E T_o}{V_e^2 \bar{\sigma}_o |\sigma_o|}$$

$$\bar{\sigma} = \frac{\sigma}{|\sigma_o|} \qquad\qquad \bar{v}_1, \bar{v}_2 = \frac{V_1}{V_2}, 1 \qquad\qquad \bar{\alpha} = \frac{\alpha T_o}{\bar{\sigma}_o}$$

$$\bar{v} = \frac{v}{V_2 \bar{\sigma}_o} \qquad\qquad \bar{v}_T, \bar{v}_e = \frac{V_T}{V_2}, \frac{V_e}{V_2} \qquad\qquad \bar{\tau} = \frac{\tau}{t_s}$$

$$\bar{\epsilon} = \frac{\epsilon}{\bar{\sigma}_o} \qquad\qquad \bar{\tau}_i = \frac{\tau_i}{t_s} \qquad\qquad \bar{k} = \frac{kT_o}{v_2^2 t_s \bar{\sigma}_o |\sigma_o|} \qquad (9a)$$

from which it also follows that

$$\bar{v}_T = \sqrt{\frac{\bar{k}}{\bar{C}_\sigma \bar{\tau}}} \qquad\qquad \delta = \frac{\bar{\alpha}^2}{\bar{C}_\sigma - \bar{\alpha}^2} \qquad\qquad \gamma = \frac{\bar{k}}{\bar{\tau}(\bar{C}_\sigma - \bar{\alpha}^2)\bar{v}_e^2} \qquad (9b)$$

The bar as used in Equations (9) will be dropped hereafter for convenience of notation, and all subsequent variables and parameters will be nondimensional. The nondimensional governing equations are then written as

$$\tau \frac{\partial Q}{\partial t} + Q = -k \frac{\partial \theta}{\partial x} \qquad (10a)$$

$$\epsilon_1 = \sigma \qquad (10b)$$

$$\frac{\partial \epsilon_2}{\partial t} = |\sigma|^n \, \text{sgn}(\sigma) \qquad (10c)$$

$$\frac{\partial \epsilon_i}{\partial t} = k_i \left[-\frac{1}{\tau_i} e^{-t/\tau_i} \int_0^t e^{-t'/\tau_i} |\sigma|^{q_i} \text{sgn}(\sigma) dt' + |\sigma|^{q_i} \text{sgn}(\sigma) \right], i=3,\ldots,N \qquad (10d)$$

$$\epsilon_T = \alpha\theta \qquad (10e)$$

$$\frac{\partial Q}{\partial x} + \alpha \frac{\partial \sigma}{\partial t} + C_\sigma \frac{\partial \theta}{\partial t} = 0 \qquad (10f)$$

$$\sum_{i=1}^N \frac{\partial \epsilon_i}{\partial t} + \frac{\partial \epsilon_T}{\partial t} = \frac{\partial v}{\partial x} \qquad (10g)$$

$$\frac{\partial \sigma}{\partial x} = \frac{1}{v_e^2} \frac{\partial v}{\partial t} \qquad (10h)$$

where $k_i = 1/\tau_i \mu_i^{q_i}$. Equations (10) are $N + 5$ first order partial differential equations in the variables $\varepsilon_i (i=1,\ldots,N)$, ε_T , Q , θ , σ and v .

3. THE METHOD OF CHARACTERISTICS

3(a). Characteristic Equations

Equations (10) are in general nonlinear and it is very difficult to obtain closed form solutions. A convenient method of approach is based upon obtaining the N + 5 base characteristics for this set of equations; solution may then be obtained by numerical integration along these characteristics. Proceeding as in [8,9], we determine the base characteristics as

$$\left(\frac{dx}{dt}\right) = \pm V_1 = \pm \left(\frac{1 + \delta + \gamma + \sqrt{(1 + \delta + \gamma)^2 - 4\gamma}}{1 + \delta + \gamma - \sqrt{(1 + \delta + \gamma)^2 - 4\gamma}}\right)^{1/2} \tag{11a}$$

$$\left(\frac{dx}{dt}\right) = \pm V_2 = \pm 1 \tag{11b}$$

and $\left(\frac{dx}{dt}\right)^{N+1} = 0$ \hfill (11c)

Along the base characteristics $dx/dt = +V_1, +V_2$ we have the characteristic conditions

$$\left(\frac{k}{\tau} - C_\sigma V_j^2\right)\left(dv - d\sigma V_j - \sum_{i=2}^{N} \frac{\partial \epsilon_i}{\partial t} V_j dt\right) - \frac{\alpha k}{\tau} d\theta V_j - \alpha dQ V_j^2$$

$$- \frac{\alpha}{\tau} QV_j^2 dt - \alpha^2 d\sigma V_j^3 = 0 \qquad\qquad , j = 1,2 \tag{12a}$$

and along $dx/dt = -V_1, -V_2$, we have the conditions

$$\left(\frac{k}{\tau} - C_\sigma V_j^2\right)\left(dv + d\sigma V_j + \sum_{i=2}^{N} \frac{\partial \epsilon_i}{\partial t} V_j dt\right) + \frac{\alpha k}{\tau} d\theta V_j - \alpha dQ V_j^2 - \frac{\alpha}{\tau} QV_j^2 dt + \alpha^2 d\sigma V_j^3 = 0$$

$$, j = 1,2 \tag{12b}$$

Also, along the remaining N+1 base characteristics $dx/dt = 0$, we require

$$d\epsilon_i = \frac{\partial \epsilon_i}{\partial t} dt \qquad , i = 1, \ldots, N \qquad (13a)$$

$$d\epsilon_T = \frac{\partial \epsilon_T}{\partial t} dt \qquad (13b)$$

In addition to the above characteristic conditions jump condition must hold across the wave fronts, i.e., across the base characteristics defined by $dx/dt = V_1$, V_2 and passing through the point $(0,0)$. Using the bracket notation for jumps $([f] = f^- - f^+)$ we may obtain from governing equations (10)

$$V_j \{ \sum_{i=1}^{N} [\epsilon_i]_j + [\epsilon_T]_j \} = - [v]_j \qquad (14a)$$

$$-[\sigma]_j = \frac{V_j}{V_e^2} [v]_j \qquad (14b)$$

$$[\epsilon_1]_j = [\sigma]_j \qquad (14c)$$

$$[\epsilon_2]_j = 0, \quad [\frac{\partial \epsilon_2}{\partial t}]_j = [|\sigma|^n \mathrm{sgn}(\sigma)]_j \qquad (14d)$$

$$[\epsilon_i]_j = 0, \quad [\frac{\partial \epsilon_i}{\partial t}]_j = k_i [|\sigma|^{q_i} \mathrm{sgn}(\sigma)]_j, \ i = 3, \ldots, N \qquad (14e)$$

$$[\epsilon_T]_j = \alpha[\theta]_j \qquad (14f)$$

$$[Q]_j - \alpha V_j [\sigma]_j - C_\sigma V_j [\theta]_j = 0, \quad [\frac{\partial Q}{\partial x}]_j + \alpha [\frac{\partial \sigma}{\partial t}]_j + C_\sigma [\frac{\partial \theta}{\partial t}]_j = 0 \qquad (14g)$$

$$[Q]_j = \frac{k}{V_j \tau}[\theta]_j, \quad \tau[\frac{\partial Q}{\partial t}]_j + [Q]_j = -k[\frac{\partial \theta}{\partial x}]_j, \quad j = 1,2 \tag{14h}$$

Note that at the leading wave front $\sigma^+ = 0$ since the rod is initially stress free, and thus the second of equations (14d,14e) simplify to

$$[\frac{\partial \varepsilon_2}{\partial t}]_1 = |[\sigma]_1|^n \text{sgn}[\sigma]_1 \tag{15a}$$

$$[\frac{\partial \varepsilon_i}{\partial t}]_1 = k_i |[\sigma]_1|^{q_i} \text{sgn}[\sigma]_1 \quad , \quad i = 3, \ldots, N \tag{15b}$$

From characteristic condition (12a) and jump conditions (14,15) (with $\sigma^+ = 0$) , we obtain a differential equation for the stress jump at the leading wave front as

$$(\frac{\tau C_\sigma V_1^2}{k} - 1)\left\{(\frac{V_e^2}{V_1^2} + 1)\frac{d[\sigma]_1}{dt} + |[\sigma]_1|^n \text{sgn}[\sigma]_1 + \sum_{i=3}^{N} k_i |[\sigma]_1|^{q_i} \text{sgn}[\sigma]_1\right\}$$
$$- \frac{\tau \alpha^2 V_1^2}{k}(\frac{2k}{k - C_\sigma \tau V_1^2} + 1)\frac{d[\sigma]_1}{dt} - \frac{\alpha^2 V_1^2}{k - C_\sigma \tau V_1^2}[\sigma]_1 = 0 \tag{16}$$

Similarly, at the lagging wave front we obtain

$$(\frac{\tau C_\sigma V_2^2}{k} - 1)\left\{(\frac{V_e^2}{V_2^2} + 1)\frac{d[\sigma]_2}{dt} + [|\sigma|^n \text{sgn}(\sigma)]_2 + \sum_{i=3}^{N} k_i [|\sigma|^{q_i} \text{sgn}(\sigma)]_2\right\}$$
$$- \frac{\tau \alpha^2 V_2^2}{k}(\frac{2k}{k - C_\sigma \tau V_2^2} + 1)\frac{d[\sigma]_2}{dt} - \frac{\alpha^2 V_2^2}{k - C_\sigma \tau V_2^2}[\sigma]_2 = 0 \tag{17}$$

3(b). Boundary Conditions and Initial Values

On the boundary $x = 0$ the stress and temperature are prescribed by step inputs; i.e., $\sigma(0,t) = H(t)$ and $\theta(0,t) = \theta_o H(t)$, where

$H(t)$ is the unit step function. From Equation (10) we then obtain on the boundary for $t \geq 0$

$$\sigma(0,t) = 1$$

$$\varepsilon_1(0,t) = 1$$

$$\varepsilon_2(0,t) = t , \qquad \frac{\partial \varepsilon_2}{\partial t}(0,t) = 1$$

$$\varepsilon_i(0,t) = \frac{1}{\mu_i q_i}(1 - e^{-t/\tau_i}), \qquad \frac{\partial \varepsilon_i}{\partial t}(0,t) = k_i e^{-t/\tau_i}, \quad i=3,\ldots,N$$

$$\varepsilon_T(0,t) = \alpha \theta_o$$

$$\theta(0,t) = \theta_o \qquad\qquad (18)$$

Note that v and Q on the boundary cannot be found directly from the above prescribed boundary condition.

We now seek to determine the initial values of all variables at $(x,t) = (0,0)$ by combining jump conditions (14) with boundary conditions (18), since this point is both on the wave front and on the boundary. We first decompose the initial stress and temperature jumps into two parts $[\sigma_o]_1$, $[\theta_o]_1$ and $[\sigma_o]_2$, $[\theta_o]_2$, which are assumed to propagate at the speeds V_1 and V_2 respectively. Thus we obtain

$$[\sigma_o]_1 + [\sigma_o]_2 = 1 \quad \text{and} \quad [\theta_o]_1 + [\theta_o]_2 = \theta_o \qquad\qquad (19)$$

from Equations (18), and then use Equations (14g,14h) to get

$$[\theta_o]_1 = \frac{\alpha\tau V_1^2}{k-C_\sigma\tau V_1^2} [\sigma_o]_1 \quad \text{and} \quad [\theta_o]_2 = \frac{\alpha\tau V_2^2}{k-C_\sigma\tau V_2^2} [\sigma_o]_2 \tag{20}$$

Equations (19,20) are then solved simultaneously to yield the following results at the initial point:

$$[\sigma_o]_1 = \frac{(k-C_\sigma\tau V_1^2)(k-C_\sigma\tau V_2^2)}{k\alpha\tau(V_1^2-V_2^2)} \theta_o - \frac{V_2^2(k-C_\sigma\tau V_1^2)}{k(V_1^2-V_2^2)} \tag{21a}$$

$$[\sigma_o]_2 = \frac{(k-C_\sigma\tau V_1^2)(k-C_\sigma\tau V_2^2)}{k\alpha\tau(V_2^2-V_1^2)} \theta_o - \frac{V_1^2(k-C_\sigma\tau V_2^2)}{k(V_2^2-V_1^2)} \tag{21b}$$

$$[\theta_o]_1 = \frac{\alpha\tau V_1^2 V_2^2}{k(V_2^2-V_1^2)} - \frac{V_1^2(k-C_\sigma\tau V_2^2)}{k(V_2^2-V_1^2)} \theta_o \tag{21c}$$

$$[\theta_o]_2 = \frac{\alpha\tau V_1^2 V_2^2}{k(V_1^2-V_2^2)} - \frac{V_2^2(k-C_\sigma\tau V_1^2)}{k(V_1^2-V_2^2)} \theta_o \tag{21d}$$

From Equations (21) and the jump conditions (14), we obtain at the leading wave

$$[v_o]_1 = - \frac{V_e^2}{V_1} [\sigma_o]_1$$

$$[\epsilon_{o1}]_1 = [\sigma_o]_1$$

$$[\epsilon_{o2}]_1 = 0, \quad [\frac{\partial\epsilon_{o2}}{\partial t}]_1 = [|\sigma|^n\text{sgn}(\sigma)]_1$$

$$[\epsilon_{oi}]_1 = 0, \quad [\frac{\partial\epsilon_{oi}}{\partial t}]_1 = k_i[|\sigma|^{q_i}\text{sgn}(\sigma)]_1, \quad i=3,\ldots,N$$

$$[\epsilon_{oT}]_1 = \alpha[\theta_o]_1$$

$$[Q_o]_1 = \frac{k}{\tau V_1} [\theta_o]_1 \tag{22}$$

Similarly, we obtain at the lagging wave

$$[v_o]_2 = -\frac{v_e^2}{V_2}[\sigma_o]_2$$

$$[\epsilon_{o1}]_2 = [\sigma_o]_2$$

$$[\epsilon_{o2}]_2 = 0, \quad [\frac{\partial \epsilon_{o2}}{\partial t}]_2 = [|\sigma|^n \text{sgn}(\sigma)]_2$$

$$[\epsilon_{oi}]_2 = 0, \quad [\frac{\partial \epsilon_{oi}}{\partial t}]_2 = k_i[|\sigma|^{q_i}\text{sgn}(\sigma)]_2, \quad i=3,\dots,N$$

$$[\epsilon_{oT}]_2 = \alpha[\theta_o]_2$$

$$[Q_o]_2 = \frac{k}{\tau V_2}[\theta_o]_2 \tag{23}$$

Finally, by combining Equations (22) with (23) we may then obtain
the desired initial values for all variables at $(x,t) = (0,0)$ as

$$\sigma(0,0) = 1$$

$$v(0,0) = -v_e^2 \left(\frac{[\sigma_o]_1}{V_1} + \frac{[\sigma_o]_2}{V_2}\right)$$

$$\epsilon_1(0,0) = 1$$

$$\epsilon_2(0,0) = 0, \quad \frac{\partial \epsilon_2}{\partial t} = 1$$

$$\epsilon_i(0,0) = 0, \quad \frac{\partial \epsilon_i}{\partial t} = k_i, \quad i = 3,\dots,N$$

$$\varepsilon_T(0,0) = \alpha\theta_o$$

$$\theta(0,0) = \theta_o$$

$$Q(0,0) = \frac{k}{\tau}(\frac{[\theta_o]_1}{V_1} + \frac{[\theta_o]_2}{V_2})\tag{24}$$

With characteristic conditions (12,13), jump conditions (14), boundary condition (18) and initial values (24), a numerical procedure for obtaining stress and temperature solutions may be established. However, closed form solutions may be obtained in some special cases, and we first develop such a solution in the next section for the uncoupled thermal wave problem. We also solve this special case by the method of characteristics, before proceeding to the numerical solution of the general problem.

4. UNCOUPLED THERMAL WAVE PROBLEM

4(a).   Closed Form Solution

For the uncoupled case we set $\alpha = 0$ in Equation (10f) and obtain the uncoupled energy equation

$$\frac{\partial Q}{\partial x} + C_\sigma \frac{\partial \theta}{\partial t} = 0 \tag{25}$$

By combining Equations (10a) with (25) we may then obtain an uncoupled thermal wave equation as

$$\frac{\partial^2 \theta}{\partial t^2} + \frac{1}{\tau} \frac{\partial \theta}{\partial t} - V_T^2 \frac{\partial^2 \theta}{\partial x^2} = 0 \tag{26}$$

where $V_T = \sqrt{k/C_\sigma \tau}$ is the uncoupled thermal wave speed. (Note that $V_T = \underset{\alpha \to 0}{\text{Lim}} \ V_2$ via Equation (6) while the uncoupled mechanical wave speed $V_e = \underset{\alpha \to 0}{\text{Lim}} \ V_1$.)   We can simplify the problem further by introducing a new set of coordinates as

$$x^* = \frac{x}{V_T \tau} \qquad t^* = \frac{t}{\tau} \tag{27}$$

Equation (26) then becomes

$$\frac{\partial^2 \theta}{\partial t^{*2}} + \frac{\partial \theta}{\partial t^*} - \frac{\partial^2 \theta}{\partial x^{*2}} = 0 \tag{28}$$

The rod is initially at uniform temperature T_o, and a step in temperature is applied on the boundary $x^* = 0$ at $t^* = 0^+$. Thus, the initial values are given in this case as

$$\theta(x^*, 0^-) = 0$$

$$\frac{\partial\theta}{\partial t^*}(x^*, 0^-) = 0 \tag{29a}$$

and the boundary condition as

$$\theta(0,t^*) = \theta_o H(t^*) \tag{29b}$$

With the use of the Laplace transform of Equations (28,29), we may obtain the solution for the temperature distribution along the rod as

$$\theta = \theta_o \left\{ \int_o^{t^*} \left[\frac{x^*}{2\sqrt{t'^2-x^{*2}}} e^{-t'/2} I_1(\tfrac{1}{2}\sqrt{t'^2-x^{*2}}) H(t'-x^*) + \frac{1}{2} e^{-t'/2} H(t'-x^*) \right] dt' \right.$$
$$\left. + e^{-t^*/2} H(t^*-x^*) \right\} \tag{30}$$

where $I_1(t)$ is the modified Bessel function of the first kind of order one. At the wave front, i.e., at $x^* = t^*$, Equation (30) reduces to

$$\theta = \theta_o e^{-t^*/2} \tag{31}$$

Also, the solution behind the wave front, i.e., for $0 \le x^* < t^*$, may be written as

$$\theta = \theta_o \left\{ \int_{x^*}^{t^*} \frac{x^*}{2\sqrt{t'^2-x^{*2}}} e^{-t'/2} I_1(\tfrac{1}{2}\sqrt{t'^2-x^{*2}}) dt' + e^{-x^*/2} \right\} \tag{32}$$

which can be readily evaluated by numerical integration.

4(b).   Numerical Solution via Method of Characteristics

Setting $\alpha = 0$ in Equations (12) we obtain the uncoupled mechanical characteristic conditions (see [5])

$$dv = \pm(d\sigma + \sum_{i=2}^{N} \frac{\partial \varepsilon_i}{\partial t} dt) \tag{33}$$

along $dx/dt = \pm V_e$ respectively, and the uncoupled thermal characteristic conditions

$$d\theta = \mp(\tau dQ + Qdt)\frac{V_T}{k} \tag{34}$$

along $dx/dt = \pm V_T$ respectively. The solution to the uncoupled mechanical wave problem by the method of characteristics has been discussed in detail by Cozzarelli and Shaw [8-10], and thus we will confine our attention to the numerical solution of the uncoupled thermal wave problem.

Equations (34) are firs as

$$d\theta = \mp(dQ^* + Q^* dt^*) \tag{35}$$

along $dx^*/dt^* = \pm 1$ respectively, where

$$Q^* = \frac{QV_T\tau}{k} \tag{36}$$

Next we note that jump condition (14h) simplifies to

$$Q^* = \theta \tag{37}$$

Combining Equations (35,37) we obtain at the uncoupled thermal wave front

$$2d\theta = -\theta dt^* \tag{38}$$

This result integrates immediately to

$$\theta = \theta_o e^{-t^*/2} \tag{39}$$

which is identical with Equation (31). Next, the boundary condition for $t^* \geq 0$ is

$$\theta(0,t^*) = \theta_o \tag{40}$$

Finally, the initial values are given by

$$\theta(0,0) = \theta_o$$

$$Q^*(0,0) = \theta_o \tag{41}$$

The equations developed in this section may be approximated by a finite difference scheme. We use mesh points at the intersections of the three base characteristic families $dx^*/dt^* = +1, -1$ and 0, which gives a constant increment $\Delta x^* = \Delta t^*$. This is shown in Figure 1. Mesh points are distinguished as wave front points, i.e., lying along the wave front $(x^* = t^*)$, boundary points, i.e.,

lying on the boundary $(x^* = 0)$, and interior points.

We use $S\Delta t^*$ to indicate the discrete values of t^* at which calculation are performed, and $(J-1)\Delta x^*$ to indicate the discrete values of x^* with $J = 1$ representing the boundary $x^* = 0$. Because of the alternating pattern of mesh points defined by the intersections of the three base characteristics, one row of constant t^* mesh points will start from the boundary $(J = 1)$ with an increment of $2\Delta x^*$ in the x^* direction until the wave front is reached, using only odd values of J. The next row will start at a mesh point $(J = 2)$ with an increment of $2\Delta x^*$ until the wave front is reached, using only even values of J. It is convenient from a computer storage point of view to condense these two rows such that one value of K, which determines two values of t^*, will contain all values of J. This is done by letting

$$t^* = S\Delta t^* = \begin{cases} 2K\Delta t^* & \text{only odd values of } J \\ \\ (2K+1)\Delta t^* & \text{only even values of } J \end{cases} \tag{42}$$

Ordinary differential equations (35) may be approximated by finite difference equations using a modified Euler method (see [11]), thus we write

$$Q = \frac{1}{2}[Q(J,S) + Q(J-1, S-1)] \tag{43}$$

The resulting algebraic equations at the interior points are given by

$$\theta(J,S)-\theta(J-1,S-1)= -Q^*(J,S)+ Q^*(J-1,S-1)- \frac{1}{2}[Q^*(J,S)+ Q^*(J-1,S-1)]\Delta t^*$$

<div align="right">(44a)</div>

along $dx^*/dt^* = +1$, and

$$\theta(J,S)-\theta(J-1,S-1)= Q^*(J,S)- Q^*(J-1,S-1)+ \frac{1}{2}[Q^*(J,S)+ Q^*(J-1,S-1)]\Delta t^*$$

<div align="right">(44b)</div>

along $dx^*/dt^* = -1$.

Equations (44) may be solved for $\theta(J,S)$ and $Q^*(J,S)$ once the previous (S-1) values are known.

For points on the boundary, $J = 1$, the boundary condition (40) will be used instead of Equation (44a). Similarly, for points on the wave front Equation (44b) is replaced by jump condition (37). In any case, the initial values (41) must be applied to start the numerical calculation. The temperature difference field $\theta(x^*,t^*)$ was calculated both by the numerical procedure outlined in this section and by the closed form solution of the previous section (Equation (30)). Identical results were obtained via the two methods, and Figure 2 shows some field solutions for θ plotted as a function of distance at several specific times ($t^* = 1,2,3$). This figure clearly shows that the use of the modified Fourier heat conduction law results in a damped thermal wave, even when damping due to viscoelastic and coupling effects are not present.

5. NUMERICAL PROCEDURE AND RESULTS
FOR THE GENERAL PROBLEM

In the general coupled case $(\alpha \neq 0)$, the coupling of the characteristic condition (12) necessitates a more complicated numerical procedure than in section 4(b). However, the method of approach for $\alpha \neq 0$ contains some similarities to that for the uncoupled case.

5(a).   Numerical Procedure

We choose $V_1 = 3$ as an illustrative example, and use a finite difference scheme with mesh points lying on the intersections of the base characteristics of the three families $dx/dt = +3, -3$ and 0. This is shown in Figure 3. Additional points along the base characteristics $dx/dt = +1$ and -1 may be obtained by linear interpolation between the mesh points, since these additional points lie within the domain of dependence of the differential equations. Mesh points in Figure 3 are distinguished as leading wave front points, i.e., lying along the leading wave front $(x = 3t)$, boundary points, i.e., lying on the boundary $(x = 0)$, lagging wave front points, i.e., lying along the lagging wave front $(x = t)$, and interior points (two types). These different types of mesh points require separate calculation routines. We use $S\Delta t$ to indicate the discrete values of t at which calculation are performed, and $(J-1)\Delta x$ to indicate the discrete values of x with $J = 1$ representing the boundary $x = 0$. A similar numerical approach but with a cruder finite difference mesh scheme was used by Lopez and Lord [12] to study the special case of coupled linear thermoelastic wave propagation with second sound.

As in the uncoupled thermal wave problem we may take advantage of the alternating pattern of the finite difference mesh to save computer storage space. We note that one row of constant t mesh points starts from the boundary $(J=1)$ with an increment of $6\Delta x$ in the x direction up to the leading wave front, using only odd values of J. The next row starts at a mesh point $(J = 4)$ with an increment of $6\Delta x$ up to the leading wave front, using only even values of J. We may condense these two rows by defining S in terms of K (see Figure 3) as

$$t = S\Delta t = \begin{cases} 2K\Delta t & \text{only odd values of } J \\ \\ (2K+1)\Delta t & \text{only even values of } J, \quad K = 0,1,2,\ldots \end{cases} \quad (45)$$

Ordinary differential equations (12,13) may be approximated by finite difference equations using a modified Euler method, i.e., we employ average values for the functions $\partial\varepsilon_1/\partial t$, $\partial\varepsilon_T/\partial t$ and Q. The resulting nonlinear algebraic equations obtained from equations (12) for interior points are given by

$$(\frac{k}{\tau} - 9C_\sigma)\left\{v(J,S)-v(J-3,S-1)-3\sigma(J,S)+3\sigma(J-3,S-1)\right.$$

$$-3\Delta t\left[\frac{\frac{\partial\varepsilon_2}{\partial t}(J,S)+\frac{\partial\varepsilon_2}{\partial t}(J-3,S-1)}{2} + \sum_{i=3}^{N}\frac{\frac{\partial\varepsilon_1}{\partial t}(J,S)+\frac{\partial\varepsilon_1}{\partial t}(J-3,S-1)}{2}\right]\right\}$$

$$-\frac{3\alpha k}{\tau}[\theta(J,S)-\theta(J-3,S-1)]-9\alpha[Q(J,S)-Q(J-3,S-1)]$$

$$-\frac{9\alpha}{\tau}\Delta t\,[\frac{Q(J,S)+Q(J-3,S-1)}{2}]- 27\alpha^2[\sigma(J,S)-\sigma(J-3,S-1)]= 0 \quad (46a)$$

along $dx/dt = +3$, and similarly

$$(\frac{k}{\tau} - 9C_\sigma)\left\{v(J,S)-v(J+3,S-1)+3\sigma(J,S)-3\sigma(J+3,S-1)\right.$$

$$+3\Delta t\left[\frac{\frac{\partial\epsilon_2}{\partial t}(J,S)+\frac{\partial\epsilon_2}{\partial t}(J+3,S-1)}{2} + \sum_{i=3}^{N}\frac{\frac{\partial\epsilon_i}{\partial t}(J,S)+\frac{\partial\epsilon_i}{\partial t}(J+3,S-1)}{2}\right]\right\}$$

$$+ \frac{3\alpha k}{\tau}[\theta(J,S)-\theta(J+3,S-1)] - 9\alpha[Q(J,S)-Q(J+3,S-1)]$$

$$- \frac{9\alpha}{\tau}\Delta t[\frac{Q(J,S)+Q(J+3,S-1)}{2}] + 27\alpha^2[\sigma(J,S)-\sigma(J+3,S-1)] = 0 \qquad (46b)$$

along $dx/dt = -3$. Also,

$$(\frac{k}{\tau} - C_\sigma)\left\{v(J,S)-v(J-1,S-1)-\sigma(J,S)+\sigma(J-1,S-1)\right.$$

$$-\Delta t\left[\frac{\frac{\partial\epsilon_2}{\partial t}(J,S)+\frac{\partial\epsilon_2}{\partial t}(J-1,S-1)}{2} + \sum_{i=3}^{N}\frac{\frac{\partial\epsilon_i}{\partial t}(J,S)+\frac{\partial\epsilon_i}{\partial t}(J-1,S-1)}{2}\right]\right\}$$

$$- \frac{\alpha k}{\tau}[\theta(J,S)-\theta(J-1,S-1)]-\alpha[Q(J,S)-Q(J-1,S-1)]$$

$$- \frac{\alpha}{\tau}\Delta t[\frac{Q(J,S)+Q(J-1,S-1)}{2}] -\alpha^2[\sigma(J,S)-\sigma(J-1,S-1)] = 0 \qquad (46c)$$

along $dx/dt = +1$, and

$$(\frac{k}{\tau} -C_\sigma)\left\{v(J,S)-v(J+1,S-1)+\sigma(J,S)-\sigma(J+1,S-1)\right.$$

$$+\Delta t\left[\frac{\frac{\partial\epsilon_2}{\partial t}(J,S)+\frac{\partial\epsilon_2}{\partial t}(J+1,S-1)}{2} + \sum_{i=3}^{N}\frac{\frac{\partial\epsilon_i}{\partial t}(J,S)+\frac{\partial\epsilon_i}{\partial t}(J+1,S-1)}{2}\right]\right\}$$

$$+ \frac{\alpha k}{\tau}[\theta(J,S)-\theta(J+1,S-1)]-\alpha[Q(J,S)-Q(J+1,S-1)]$$

$$- \frac{\alpha}{\tau} \Delta t [\frac{Q(J,S)+Q(J+1,S-1)}{2}] + \alpha^2 [\sigma(J,S) - \sigma(J+1,S-1)] = 0 \qquad (46d)$$

along $dx/dt = -1$. Finally, equations (13) yield

$$\varepsilon_1(J,S) - \varepsilon_1(J,S-2) = 2 \Delta t \left[\frac{\frac{\partial \varepsilon_1}{\partial t}(J,S) + \frac{\partial \varepsilon_1}{\partial t}(J,S-2)}{2} \right] \qquad (46e)$$

$$\varepsilon_2(J,S) - \varepsilon_2(J,S-2) = 2 \Delta t \left[\frac{\frac{\partial \varepsilon_2}{\partial t}(J,S) + \frac{\partial \varepsilon_2}{\partial t}(J,S-2)}{2} \right] \qquad (46f)$$

$$\varepsilon_i(J,S) - \varepsilon_i(J,S-2) = 2 \Delta t \left[\frac{\frac{\partial \varepsilon_i}{\partial t}(J,S) + \frac{\partial \varepsilon_i}{\partial t}(J,S-2)}{2} \right], \quad i=3,\dots,N \quad (46g)$$

$$\varepsilon_T(J,S) - \varepsilon_T(J,S-2) = 2 \Delta t \left[\frac{\frac{\partial \varepsilon_T}{\partial t}(J,S) + \frac{\partial \varepsilon_T}{\partial t}(J,S-2)}{2} \right] \qquad (46h)$$

along $dx/dt = 0$. Nonlinear algebraic equations (46a-h) may be solved for v, σ, ε_i, $\partial \varepsilon_i / \partial t$, θ, Q, ε_T, and $\partial \varepsilon_T / \partial t$ for mesh points at a given S once the previous $(S-1)$ values are known.

The methods used to obtain solutions at the various types of mesh points shown in Figure 3 are summarized below.

(i) Initial Point: All initial values are given by Equations (21-24).

(ii) Leading Wave Front Points: Stress is obtained by integrating Equation (16), and the remaining variables are obtained from Equations (14).

(iii) First Boundary Point (see Figure 4a): At the initial point $(0,0)$ all $N + 5$ variables are known from Equations (24). At the first boundary point $(0,2)$ we know the values of all variables except v and Q from Equations (18). We start an iteration process

for determining the values of v and Q by first setting v and Q at point $(0,2)$ equal to their values at point $(0,0)$. We interpolate for values of any variable at point 1 using the values at points $(0,0)$ and $(0,2)$. At point 4 all variables are known from the previous time step. The jumps of all variables at points 2 and 6 are obtained from the integration of Equation (17) and jump conditions (14) (see enlarged Figure 4b). Basing on linear interpolation and the assumption that the slope of any variable at the lagging wave front will remain the same as it crosses the wave front, we obtain

$$②=(① - [2] - ④) \times \frac{2}{3} + ④ + [2]$$

$$③=(① - [2] - ④) \times \frac{1}{3} + ④$$

$$⑤=(① - [2] - ④) \times \frac{1}{2} + ④ \tag{47}$$

where ① indicates the value of a variable at point 1, and [2] represents the jump across the lagging wave front at point 2. Once all values of the variables at points (1-5) are obtained, we may use Equations (14,46) to solve for the $N + 5$ variables at point 6. From points 2 and 6 and Equations (46b,46d) we may then find an improved value of v and Q at point $(0,2)$. By this procedure we may obtain v and Q at point $(0,2)$ through iteration.

(iv) Subsequent Boundary Points (see Figure 5): First we assume values for v and Q at point $(0,S)$. Then we interpolate point 1 from points $(0,S-2)$ and $(0,S)$. We know point 3 from previous time steps. Therefore, point 2 can be obtained from points 1 and 3 via

linear interpolation. Finally we may evaluate the values of v and Q at point $(0,S)$ from points 2 and 3 from Equations (46b,46d) and iteration as in part (iii).

(v) Lagging Wave Front Points (see Figure 6): The values of the $N + 5$ variables at points 1, 4 and 5 are known from previous time steps. The jumps at points 2 and 6 can be obtained from Equations (14,17). The values of the variables at points 2 and 3 can be found by linear interpolation. The information needed to evaluate point 6 from equations (46) is then complete.

(vi) Interior Points - Type A (see Figure 7): We know the values of all variables at points 1, 7 and 9 from previous time steps, and the jumps at points 4 and 8 are obtained from Equations (14,17). We then use linear interpolation to obtain points 2, 3, 4, 5 and 6. Point 8 may then be obtained from points 3, 4, 5, 6 and 7 as in part (v). Once points 1, 2, 4, 8 and are known, we may evaluate point 10 from Equations (46).

(vii) Interior Points - Type B (see Figure 8): The values of all variables are known at points 1, 4 and 5, and points 2, 3 can be obtained from linear interpolation. Once points 1, 2, 3, 4 and 5 are known, we then have all information necessary to solve for point 6.

In the next section we present some numerical results with $V_1 = 3$ for several illustrative cases, as obtained from a computer program written for the CYBER 173. For arbitrary V_1 the lagging wave front point is not necessarily a mesh point, but values at the point may still be easily calculated via linear interpolation.

5(b). Discussion of Results

Although the program written can be employed for various generalized Kelvin material models with up to twelve elements (i.e., one linear elastic spring, one nonlinear dashpot and ten nonlinear Kelvin elements), only three material models will be discussed here. These models are the linear Maxwell model (n = 1), a nonlinear Maxwell model (n = 3) and the linear Maxwell-Kelvin model. These three models are sufficient to illustrate the effects of second sound, thermo-mechanical coupling and nonlinear viscoelastic damping. Also, all models will be solved with a positive applied step stress at the boundary, but with a zero temperature increment (i.e., $\theta_o = 0$). An applied constant tensile stress will cause the temperature to tend to drop at the boundary, and thus heat must be continuously added at x = 0 to maintain θ at zero.

In selecting a set of illustrative values for the nondimensional material constants k, τ, C_σ and α, we seek a case in which coupling and second sound are significant effects. However, on physical grounds we would still expect in general that in heat conduction equation (10a) $k \frac{\partial Q}{\partial x} > \tau \frac{\partial Q}{\partial t}$ and also that in energy equation (10f) $C_\sigma \frac{\partial \theta}{\partial t} > \alpha \frac{\partial \sigma}{\partial t}$. Thus we will choose $k > \tau$ and $C_\sigma > \alpha$, where this latter condition also ensures non-negative values for δ and γ [see Equation (9b)]. Furthermore, we must also satisfy conditions (6b) which in nondimensional form becomes for the present case $V_1 = 3 > V_T > V_e > V_2 = 1$, thereby ensuring that the leading wave be predominantly thermal. In consideration of the above we select k = 1.0, τ = 0.3, C_σ = 0.7 and α = 0.5, which then yields δ = 0.555, γ = 5.818, V_T = 2.182 and V_e = 1.273 via Equations (9b, 11a). All numerical results obtained

using these values were checked by substitution into the governing

equations with the use of the five-point finite difference derivative

formula

$$f'_o = \frac{1}{12h} (f_{-2} - 8f_{-1} + 8f_1 - f_2) + \frac{h^4}{30} f^v(\xi) \tag{48}$$

where f'_o is the first derivative of f at the central point, h

is the increment, and the last term is the truncation error.

For the first case of a linear Maxwell model, Figures 9 and 10

give the field solutions for the nondimensional stress and temperature

difference respectively as functions of distance at times $t = 0.5, 1.5$.

We see from these two figures that second sound results in two wave

fronts with finite speeds along which both the mechanical and thermal

disturbances propagate. Note that the stress (Figure 9) decreases

monotonically from the boundary value of 1.0 to a value behind the lag-

ging wave front. After a negative jump the stress again decreases

monotonically to a value behind the leading wave front. Upon compar-

ing these stresses with similar results from uncoupled theory in [10],

we find that thermomechanical coupling is a damping effect which

results in a faster relaxation of the stress jumps. The temperature

difference (Figure 10) decreases from the prescribed boundary value

to a value behind the lagging wave front. After a negative jump at

the lagging wave front it increases to a value at the leading wave

front, which is less than the initial value of zero. The temperature

difference solution in the uncoupled case for this problem is zero

everywhere.

These figures show that the damping effect due to thermomechanical

coupling and viscoelastic material behavior results in exponential decay

of all jumps at the two wave fronts. The stress jump at the leading wave front is much smaller than that at the lagging wave front, which is as expected for a mechanical input. The difference in magnitude between the two temperature jumps is not significant, but we see that they are of opposite sign. Also we see that at the lagging wave front the stress and temperature jumps are of the same sign, while at the leading wave front they are of opposite sign. In general, Figure 10 indicates that the bulk of the thermal energy is carried by the lagging wave front for a mechanical input of this type. A similar result was obtained in [12] for a linear thermoelastic material.

Figures 11 and 12 give the results for the nonlinear Maxwell model with $n = 3$. On comparing Figures 9 and 11 we see that increasing n results in a slower relaxation of the stress field. This follows from constitutive equation (10c), since as n increases, with $|\sigma| \leq 1$, the effective viscosity of the dashpot increases. More energy will be expended in displacing a dashpot as n increases, and accordingly Figure 12 shows a greater temperature drop than does Figure 10.

Finally, the solutions for the linear Maxwell-Kelvin model with $\tau = \mu = q = 1$ are shown in Figures 13 and 14. We note by comparison with Figure 9 that adding a linear Kelvin element to a linear Maxwell element results in a faster relaxation of the stress field. This is clearly due to the additional viscoelastic damping caused by the Kelvin element. This damping effect also results in a smaller temperature drop than for the linear Maxwell model, as shown in Figure 14.

6. BRIEF SUMMARY

In order to ensure a finite speed of propagation for a thermal disturbance, a modified Fourier heat conduction law was used. A one-dimensional single integral nonlinear thermoviscoelastic constitutive relation and a linearized thermomechanically coupled energy equation were also employed. Using these relations together with the one-dimensional strain-displacement relation and the equation of motion, the one-dimensional wave propagation problem was then studied for a semi-infinite rod.

Due to the nonlinearity and general complexity of the governing equations, a numerical approximation based on the method of characteristics was employed to obtain the field solutions for stress and temperature. Two thermomechanically coupled wave fronts with finite speeds were generated along the positive axis by applied step stress and temperature inputs at the boundary. A closed-form solution in integral form was obtained via the method of Laplace Transformation for the special case of an uncoupled thermal wave. A numerical solution based on the method of characteristics was also obtained in this case.

For the general coupled case, the initial values were obtained from a decomposition of the initial input and from the jump conditions. A finite difference approximation using the modified Euler method was used for the nonlinear characteristic equations. Then the field solutions were obtained from these nonlinear algebraic equations via iteration. A detailed discussion of the numerical procedure was given. Numerical results were given and discussed for three viscoelastic models.

REFERENCES

1. Rogers, S. J.: "Transport of Heat and Approach to Second Sound in Same Isotopically Pure Alkali-Halide Crystals." Phys. Review, Vol. 3, 1440-1457 (1971).

2. Chester, M.: "Second Sound in Solids." Phys. Review, Vol. 131, 2013-2015 (1963).

3. Lord, H. W., and Y. Shulman: "A Generalized Dynamical Theory of Thermoelasticity." J. Mech. Phys. Solids, Vol. 15, 299-309 (1967).

4. Achenbach, J. D.: "The Influence of Heat Conduction on Propagating Stress Jumps." J. Mech. Phys. Solids, Vol. 16, 273-282 (1968).

5. Chang, W. P., and F. A. Cozzarelli: "On the Thermodynamics of Nonlinear Single Integral Representations for Thermoviscoelastic Materials with Application to One-Dimensional Wave Propagation." Acta Mechania, Vol. 25, 187-206 (1977).

6. Cost, T. L.: "A Free Energy Functional for Thermorheologically Simple Materials." Acta Mechanica, Vol. 17, 153-167 (1973).

7. Kaliski, S.: "Wave Equations of Thermoelasticity." Bull. Acad. Polon. Sci. Ser. Sci. Tech., Vol. 13, 253-260 (1965).

8. Shaw, R. P., and F. A. Cozzarelli: "Stress Relaxation at Wave Fronts in One-Dimensional Media Described by Nonlinear Viscoelastic Models." Int. J. Nonlinear Mech., Vol. 5, 171-182 (1970).

9. Shaw, R. P., and F. A. Cozzarelli: "Wave-Front Stress Relaxation on a One-Dimensional Nonlinear Inelastic Material with Temperature and Position Dependent Properties." J. Appl. Mech., Vol. 38, 47-50 (1971).

10. Cozzarelli, F., and R. P. Shaw: "Stress, Strain and Velocity Field in a Suddenly Loaded Semi-Infinite Rod of Material Described by Non-Linear Viscoelastic Models." D.I.S.R. Report No. 29, State University of New York at Buffalo, August (1968).

11. Courtine, D., F. A. Cozzarelli and R. P. Shaw: "Effect of Time Dependent Compressibility on Non-Linear Viscoelastic Wave Propagation." Int. J. Non-Linear Mech., Vol. 11, 365-383 (1976).

12. Lopez, A. A., and H. W. Lord: "A Study of Thermoelastic Waves by the Method of Characteristics." Devel. Theo. Appl. Mech., Vol. 5, 417-447 (1971).
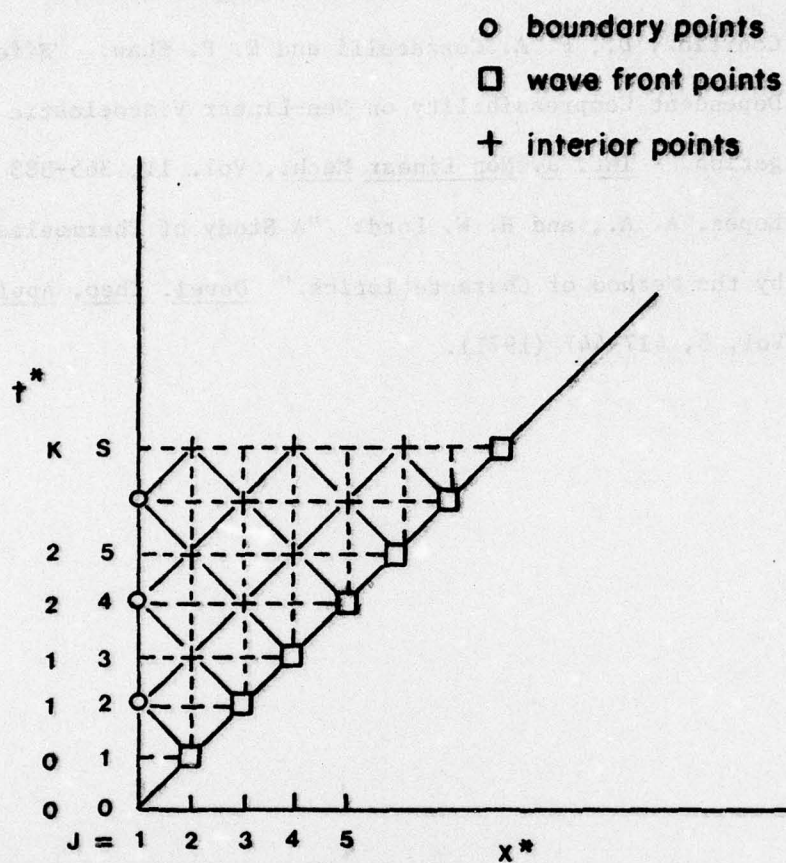
Figure 1: Grid for Numerical Integration,
Uncoupled Thermal Case
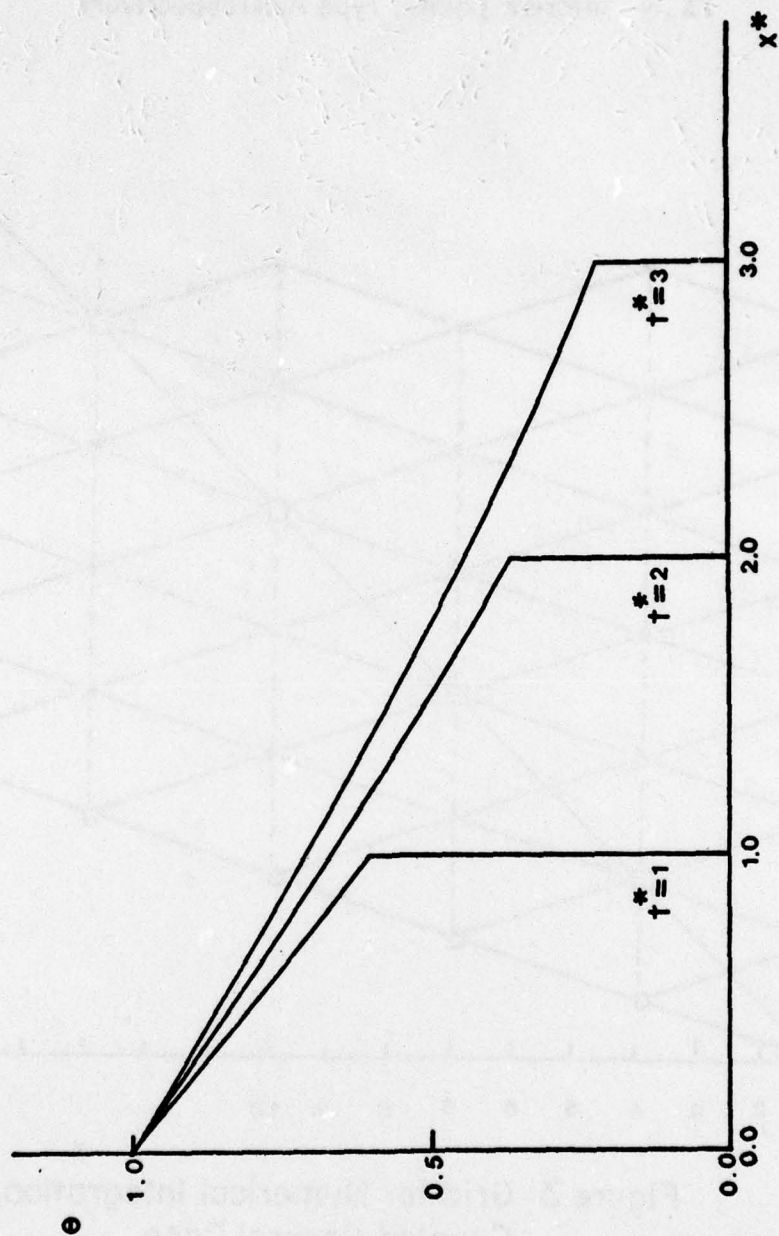
Figure 2: Uncoupled Thermal Wave, θ vs. Distance, At $t^* = 1, 2, 3$
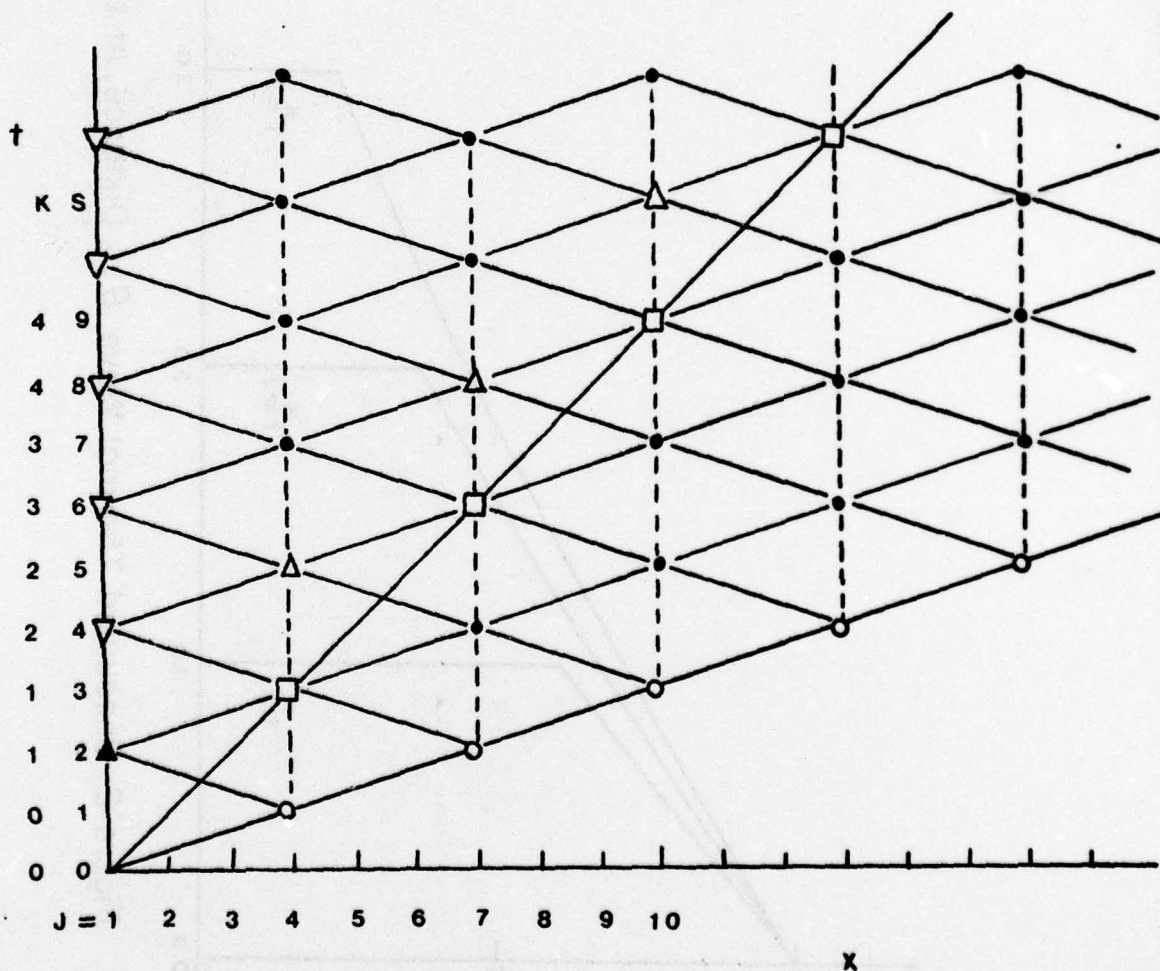
Figure 3: Grid for Numerical Integration,
Coupled General Case

(a)

(b)
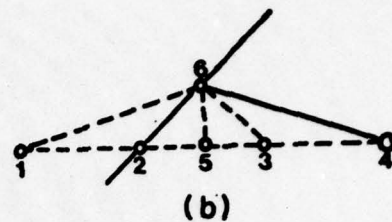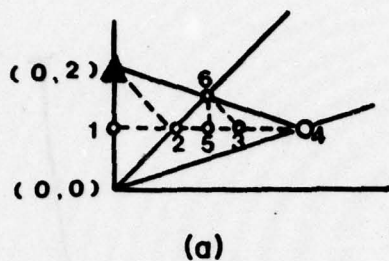
Figure 4   First Boundary Point
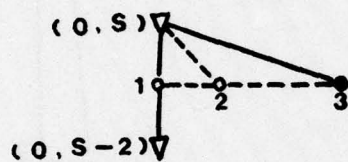
Figure 5

Subsequent Boundary Point
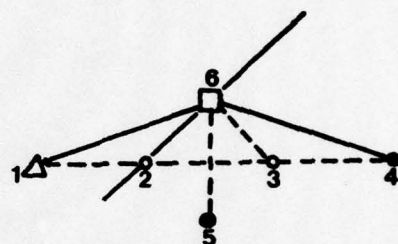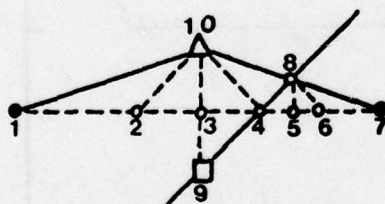
Figure 6

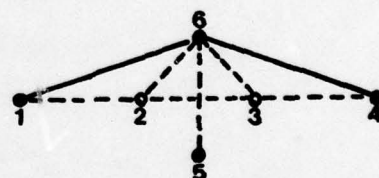Lagging Wave Front Point

Figure 7

Interior Point – Type A

Figure 8

Interior Point – Type B

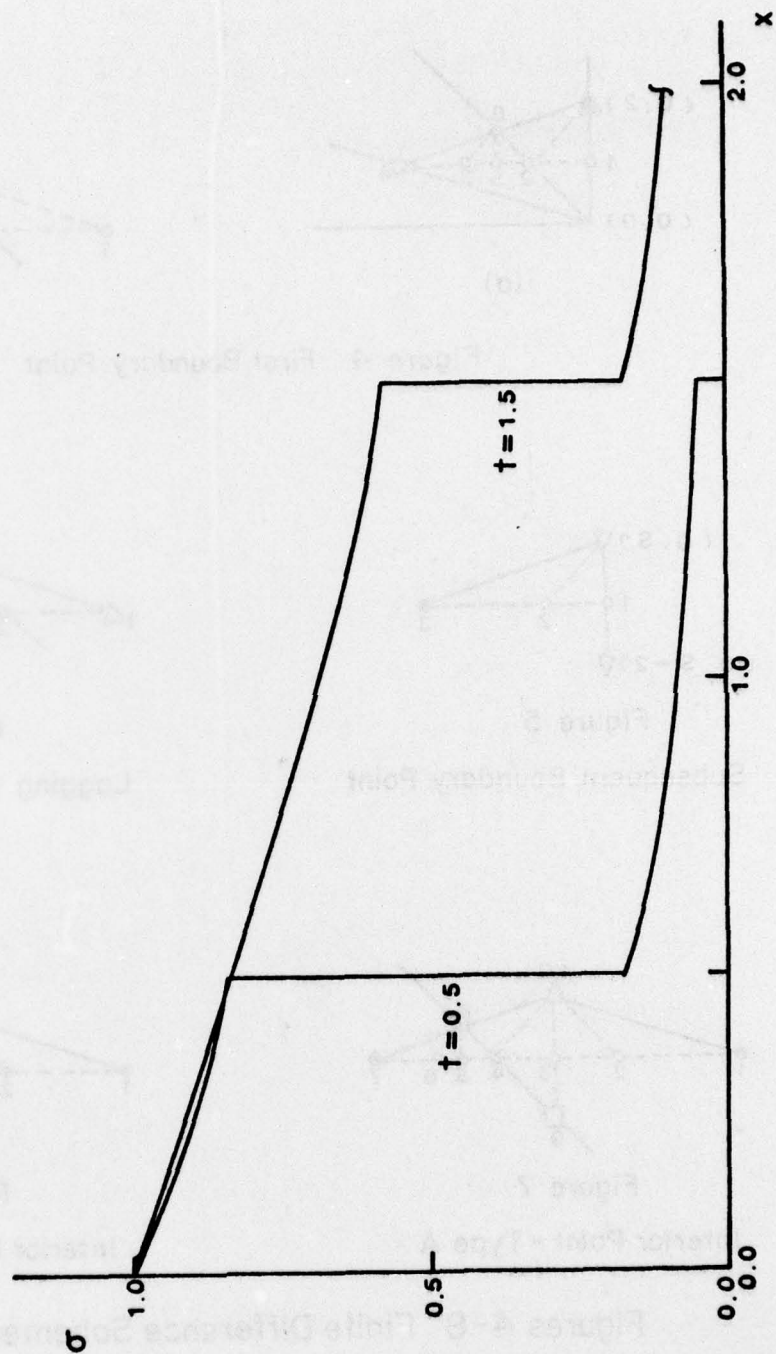Figures 4-8   Finite Difference Schemes –
Various Types of Grid Points

Figure 9: Linear Maxwell, $n = 1$, σ vs. Distance, At $t = 0.5, 1.5$
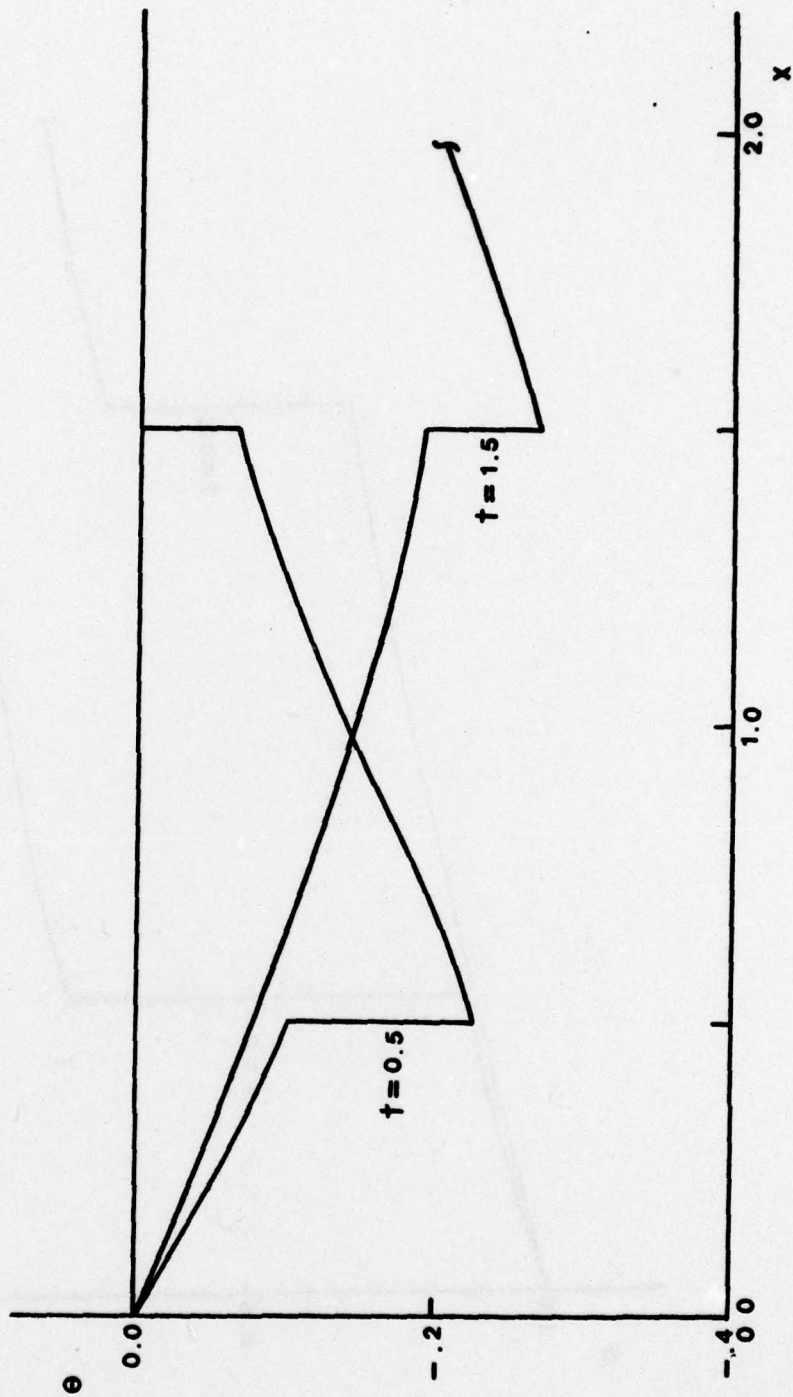
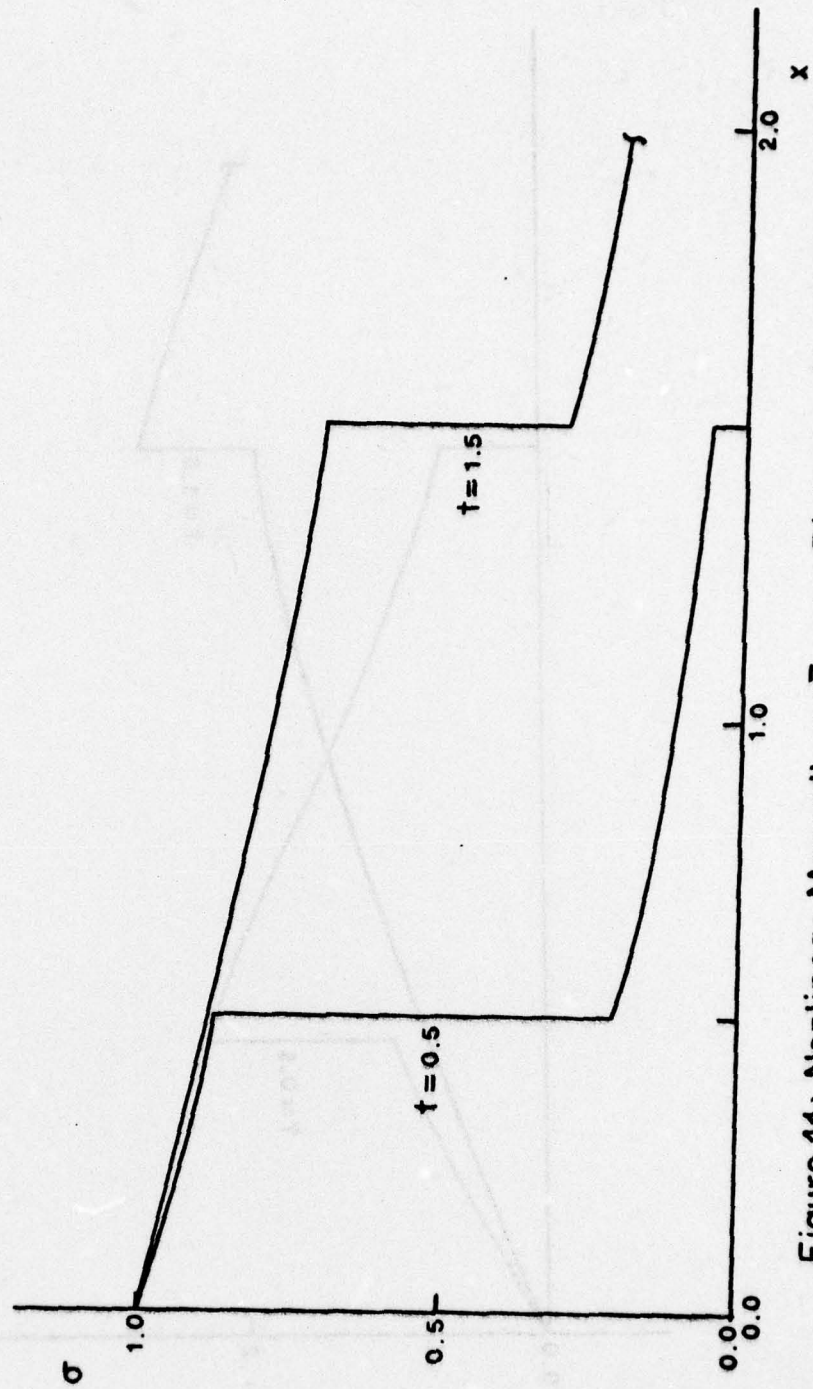Figure 10: Linear Maxwell, n=1, θ vs. Distance, At t=0.5, 1.5

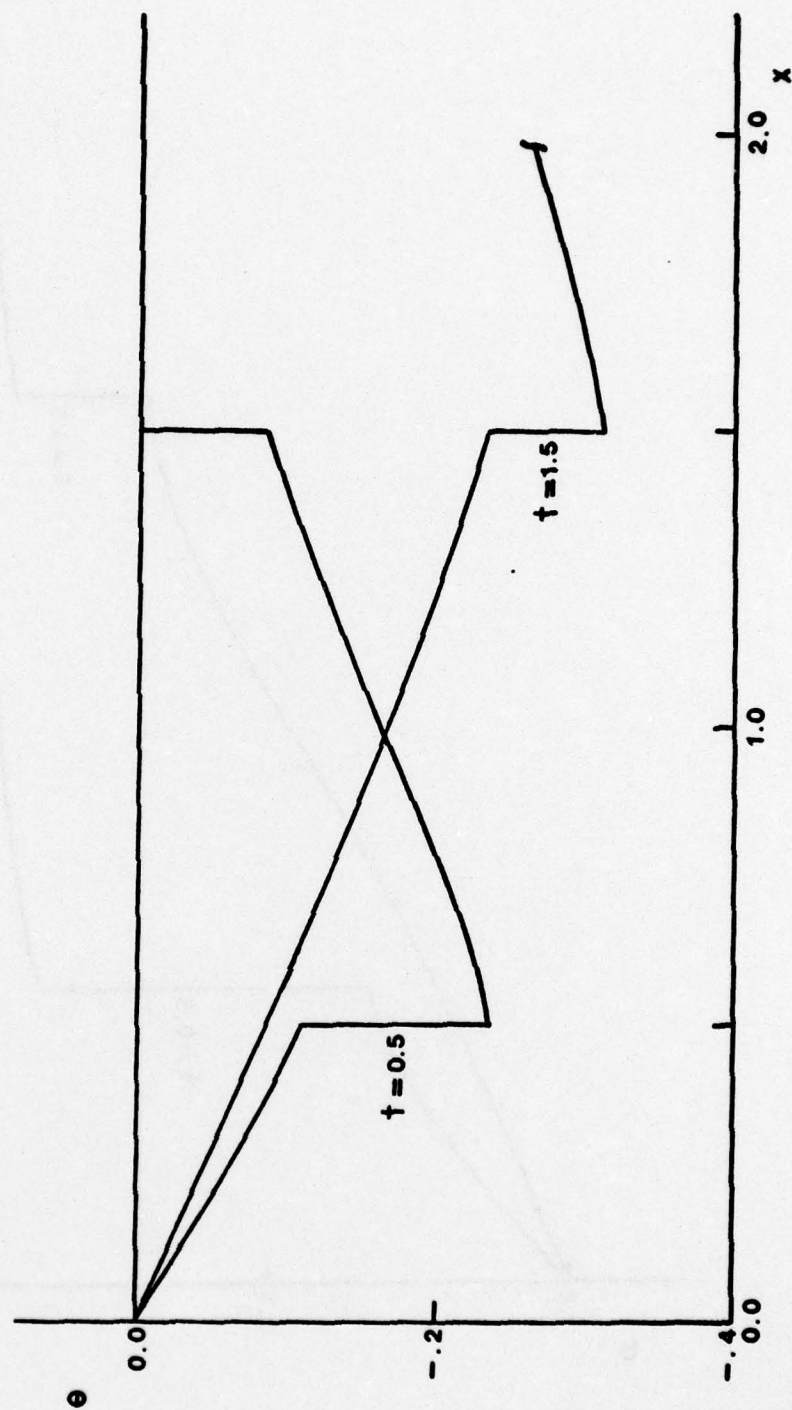Figure 11: Nonlinear Maxwell, $n = 3$, σ vs. Distance, At $t = 0.5, 1.5$

Figure 12: Nonlinear Maxwell, $n=3$, θ vs. Distance, At $t=0.5, 1.5$
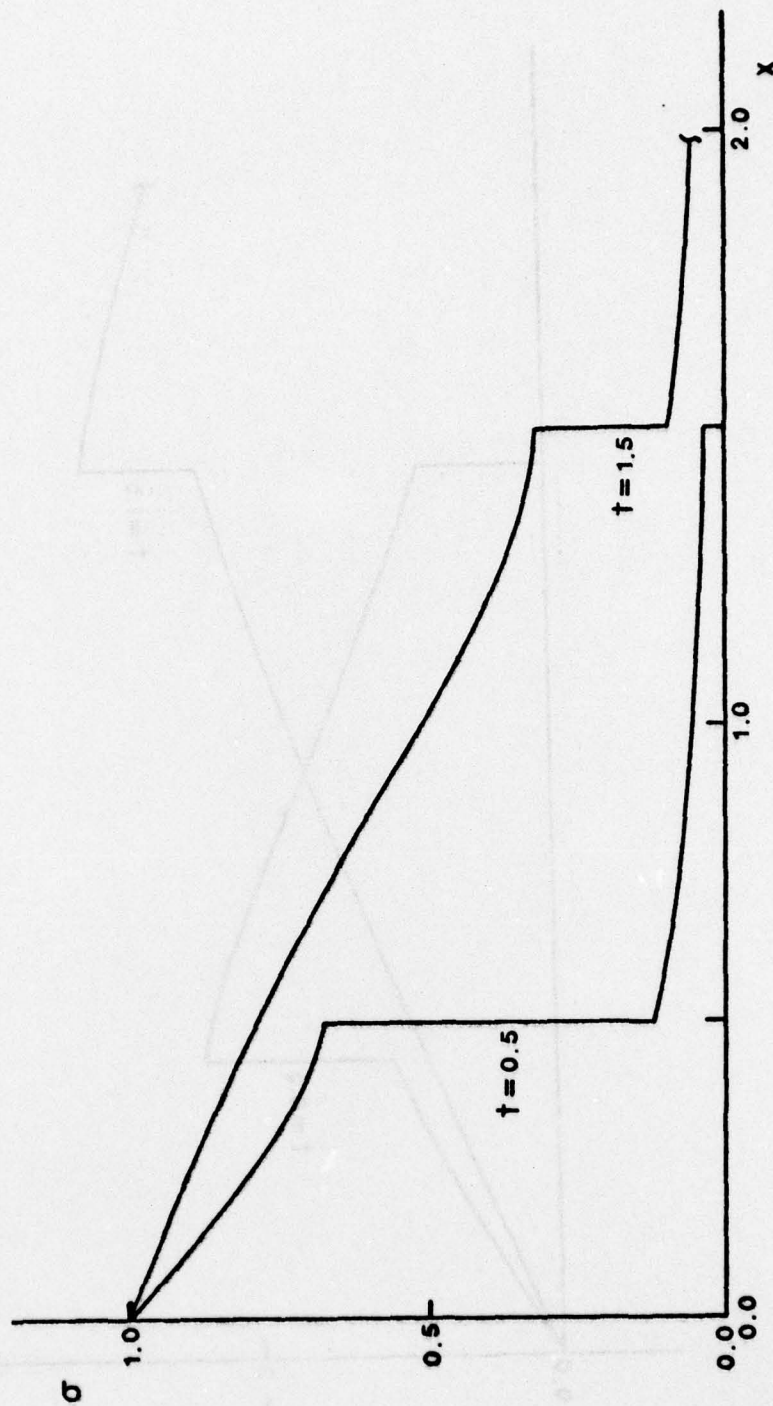
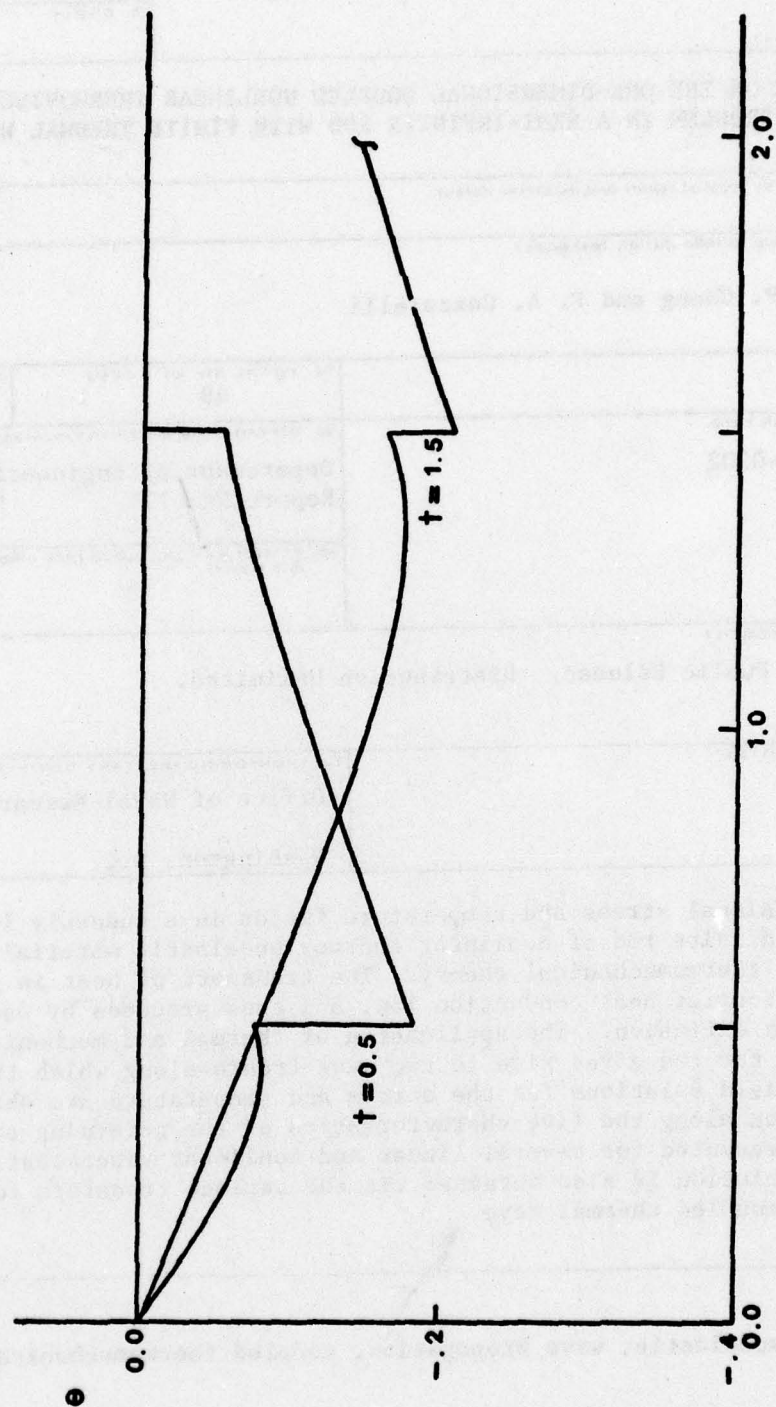Figure 13: Linear Maxwell - Kelvin, $\tau = \mu = q = 1$, σ vs. Distance, At t=0.5,1.5

-42-

Figure 14: Linear Maxwell – Kelvin, $\tau = \mu = q = 1$, θ vs. Distance, At $t = 0.5, 1.5$

DOCUMENT CONTROL DATA - R & D

Security classification of title, body of abstract and indexing annotation must be entered when the overall report is classified)

1. ORIGINATING ACTIVITY (Corporate author)	2a. REPORT SECURITY CLASSIFICATION
The Research Foundation of the State University of New York	Unclassified
	2b. GROUP

3. REPORT TITLE

SOME RESULTS ON THE ONE-DIMENSIONAL COUPLED NONLINEAR THERMOVISCOELASTIC WAVE PROPAGATION PROBLEM IN A SEMI-INFINITE ROD WITH FINITE THERMAL WAVE SPEED

4. DESCRIPTIVE NOTES (Type of report and inclusive dates)
Summary

5. AUTHOR(S) (First name, middle initial, last name)

C. Lee , W. P. Chang and F. A. Cozzarelli

6. REPORT DATE	7a. TOTAL NO. OF PAGES	7b. NO. OF REFS
July, 1978	49	12

8a. CONTRACT OR GRANT NO.	9a. ORIGINATOR'S REPORT NUMBER(S)
N 00014-75-C-0302	Department of Engineering Science Report No. 104
b. PROJECT NO.	
c.	9b. OTHER REPORT NO(S) (Any other numbers that may be assigned this report)
d.	

10. DISTRIBUTION STATEMENT

Approved for Public Release. Distribution Unlimited.

11. SUPPLEMENTARY NOTES	12. SPONSORING MILITARY ACTIVITY
	Office of Naval Research - Structural Mechanics Washington, D.C.

13. ABSTRACT

One-dimensional stress and temperature fields in a suddenly loaded and/or heated semi-infinite rod of nonlinear thermoviscoelastic material are studied using coupled thermomechanical theory. The transport of heat is governed by the modified Fourier heat conduction law, and thus proceeds by wave propagation rather than by diffusion. The application of thermal and mechanical disturbances at the end of the rod gives rise to two wave fronts along which these disturbances propagate. Field solutions for the stress and temperature are obtained by numerical integration along the five characteristics of the governing equations, and results are presented for several linear and nonlinear viscoelastic models. A closed form solution is also obtained via the Laplace transform for the special case of an uncoupled thermal wave.

14. KEY WORDS

Nonlinear viscoelastic, wave propagation, coupled thermomechanical, second sound

DD FORM 1473 (PAGE 1)
1 NOV 65

S/N 0101-807-6811

406 156

Unclassified
Security Classification